



ORIGINAL ARTICLE

Digital Wood: 3D Internal Color Texture Mapping

Fabian Stute, Joni Mici, Lewis Chamberlain, and Hod Lipson

Abstract

Multicolor three-dimensional (3D) printing is typically used for external color textures wrapped around a monomaterial core. Here, we present a digital manufacturing workflow comprising destructive tomographic imaging and voxel printing, to replicate both the surface color texture and the internal color texture of anisotropic organic materials such as wood. Wooden samples were sliced at $27\ \mu\text{m}$ intervals and were imaged using a camera-equipped computer numerical control (CNC) mill. The resulting stack of 230 images was prepared for manufacturing on a voxel-capable 3D printer using a stochastic dithering algorithm. The final printed object closely resembles the original wooden block both in its external appearance and in its internal color pattern, as confirmed when the block is cut or broken. The presented workflow can be employed in digital replication of objects with complex internal patterns that have thus far been impossible to manufacture.

Keywords: 3D printing, voxels, bitmap printing, multimaterial, digital fabrication, texture mapping

Introduction

RECENT ADVANCES IN three-dimensional (3D) printing technology include cheaper printers, faster manufacturing processes, and the introduction of new materials. In the multimaterial manufacturing realm, established technologies include Hewlett Packard's Multi Jet Fusion and Stratasys PolyJet, both of which utilize inkjet-like technology to harmoniously mix dissimilar materials within the same part.^{1,2} More importantly, these technologies may facilitate printing with voxels—a relatively unexplored 3D printing process that allows controlling the color and material structure at every resolvable point of a printed object. In both Multi Jet Fusion and PolyJet printing, a voxel is defined as the smallest discernible physical element in a 3D-printed assembly.²

Compared with Multi Jet Fusion, PolyJet has a smaller material selection as it is limited to photoacrylates; however, it is a more mature and established additive manufacturing process. A PolyJet printer mixes dissimilar acrylates to print as many as 360,000 unique colors in durometers ranging from Shore A 27 to Shore A 85. In 2018, Stratasys introduced GrabCAD Voxel Print, a software that grants users voxel-level control of voxel placement. Such voxel-level control enables the manufacture of materials with continuous stiffness changes, often referred to as graded materials. However, the interaction between high and low durometer resins is

highly nonlinear, and can be difficult to simulate and design for. Voxel-level control also enables the manufacture of materials whose properties can be tuned in software before printing. These types of materials are often referred to as tunable materials.³ While the varying properties of graded and tunable materials offer new possibilities for optimization and multiuse parts, both of these materials cannot be accurately represented in contemporary computer-aided design (CAD) systems.⁴

Until recently, inkjet-style 3D printing technologies have been successfully utilized in the manufacture of parts with complex topologies and full color surface textures. However, these printers have struggled with parts that have anisotropic internal structures as seen in many organic materials. This drawback stems from inherent incompatibility of delivering dissimilar materials to every resolvable point of an object being printed with established 3D printing processes, such as selective laser sintering and fused deposition modeling. As of early 2018, voxel printing is possible on both the HP and Stratasys printers mentioned previously; however, preparing files for voxel printing is a challenge left largely unaddressed by printer manufacturers. One reason for this gap is that voxel printing files tend to be labor intensive to generate and computationally intensive to preprocess. Moreover, common file formats such as Standard Tessellation Language (STL) fare poorly at representing complex, voxel-based topologies.⁵⁻⁷

Department of Mechanical Engineering, Columbia University, New York, New York.

Opposite page: A digitally replicated piece of wood printed on a Stratasys J750 3D printer, shattered in liquid nitrogen. *Photo Credit:* JD Blutinger.

It follows that the lack of design tools and printing processes combines to highlight a research gap in the present-day 3D printing: the inability to replicate 3D objects with complex internal textures. This inability to print with dissimilar materials can be overcome by voxel printing, which permits printing structures with both internal grains and external color textures. Ultimately, it is envisaged that voxel printing processes will enable the manufacture of multi-material parts with complex internal structures, such as bone and wood, by delivering different types of voxels to each and every resolvable point of the fabricated object.

As voxel printing results in intricately arranged material particles throughout the resulting object, it offers designers nearly limitless manufacturing possibilities. However, to fully exploit its immense potential, the design tools and paradigms must be updated accordingly. For example, the full tray of a Stratasys J750 PolyJet printer can have as many as 760 billion individual voxels. Presently, neither design paradigms nor design tools are equipped to handle such a design environment.

As the most widely utilized design tools, commercially available CAD programs have been developed for designing monomaterial parts produced using traditional top-down manufacturing techniques. As a result, boundary representation of objects—a representation method ill suited for complex topologies and voxel-based point-cloud representations—is typically employed. Such boundary representations provide little value to designs where every small bit of matter must be specified. Bitmap-based design specifications have emerged as the *de facto* standard of voxel design and information flow. Using bitmap-based workflows, previous literature covers the digital fabrication of anisotropic, heterogeneous, bioinspired parts. Documentation of such a bitmap-based workflow is presented by Doubrovski *et al.*,⁸ delineating the manufacture of prosthetic parts with heterogeneous properties. Additional literature by Bader *et al.*⁹ and Oxman *et al.*¹⁰ reports on digital fabrication of heterogeneous objects and a rapid prototyping platform for variable elasticity, respectively. On the computa-

tional side, Aage *et al.*¹¹ report on topology optimization strategies for giga voxel-class design spaces.

Recent CAD entrants such as nTopology, NetFabb, Vox-CAD, Uformia, MeshMixer, and GrabCAD Voxel Print are examples of developmental efforts to enable the manufacture of complex topologies and voxel-based parts.^{12–14} Yet, these tools are unable to exploit the full potential of voxel printing. Currently, much of the voxel printing workflow is still left to the designer who is required to be adept at a variety of disparate software tools and processes, such as destructive imaging, pixel manipulation, and microstructure design.

In this study, voxel printing was utilized to replicate both external and internal color textures of an olive wood sample. The digitally fabricated sample is shown in Figure 1. The process consisted of removing consecutive thin slices from the wooden sample and capturing digital images of each slice. This approach resulted in a stack of images, which were postprocessed using photoediting software, before being input into a Stratasys J750 3D printer capable of printing at the voxel level. The printer replicated the wooden sample by sequentially printing layers corresponding to the image stack. The workflow before printing is described in the Materials and Methods section, while the printed samples are shown and explained in the Results section. The main findings are summarized in the Discussion section, while the implications that voxel printing workflow can have on digital manufacturing and design are delineated in the Conclusions section.

Materials and Methods

Destructive imaging

Olive wood is a material germane to this study, as it is easily machined, yet exhibits anisotropies that closely map to its visual properties. In preparation for the printing process, wooden samples were sliced using a 3040T desktop computer numerical control (CNC) mill and were imaged with an overhead camera, which allowed capturing consecutive slices of wood as

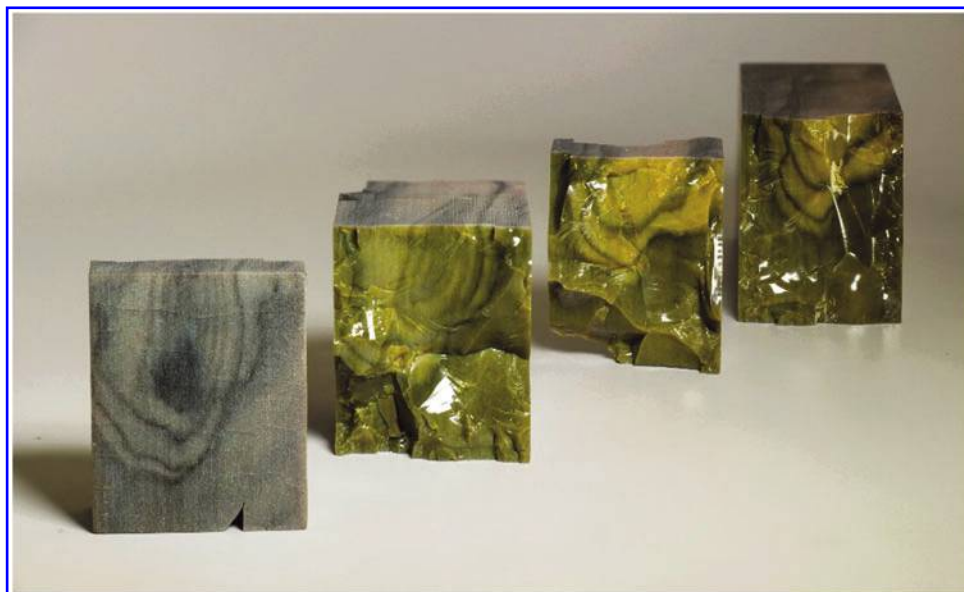


FIG. 1. A digitally replicated piece of wood printed on a J750 printer, shattered in liquid nitrogen.

they were cut (Fig. 2A). The CNC mill was controlled by a RAMBO open-sourced controller board, and both the camera and the CNC were controlled by a top-level Python script.

Material was removed from the wooden samples using a fly-cutter, which shaves $27\ \mu\text{m}$ off the wood surface in each pass (Fig. 2A). This thickness corresponds to the height of a single layer on a Stratasys J750 PolyJet 3D Printer in the High Mix setting. Upon completion of each fly-cutter pass, the overhead camera recorded a red, green, and blue (RGB) image of the newly exposed surface. This process was repeated 230 times, resulting in a stack of 230 distinct images. A selection of these images is shown in Figure 2B–H, and the full image set is provided online.¹⁵ Since images were taken in RGB format, and most printers operate on cyan, magenta,

yellow, and black (CMYK) format, the image stack was postprocessed before 3D printing.

Image postprocessing

Images were cropped to show only the wood sample cross-section. The resulting images were subsequently scaled to match the xy resolution of the Stratasys J750 printer of 600×300 pixels per inch (Fig. 2J). Image scaling was performed by invoking the MATLAB implementation of a bicubic interpolation algorithm, which uses the weighted average of four translated pixel values for each output pixel value.¹⁶ Bicubic interpolation was chosen because it produced smooth, natural color gradients, as seen in Figure 2J.

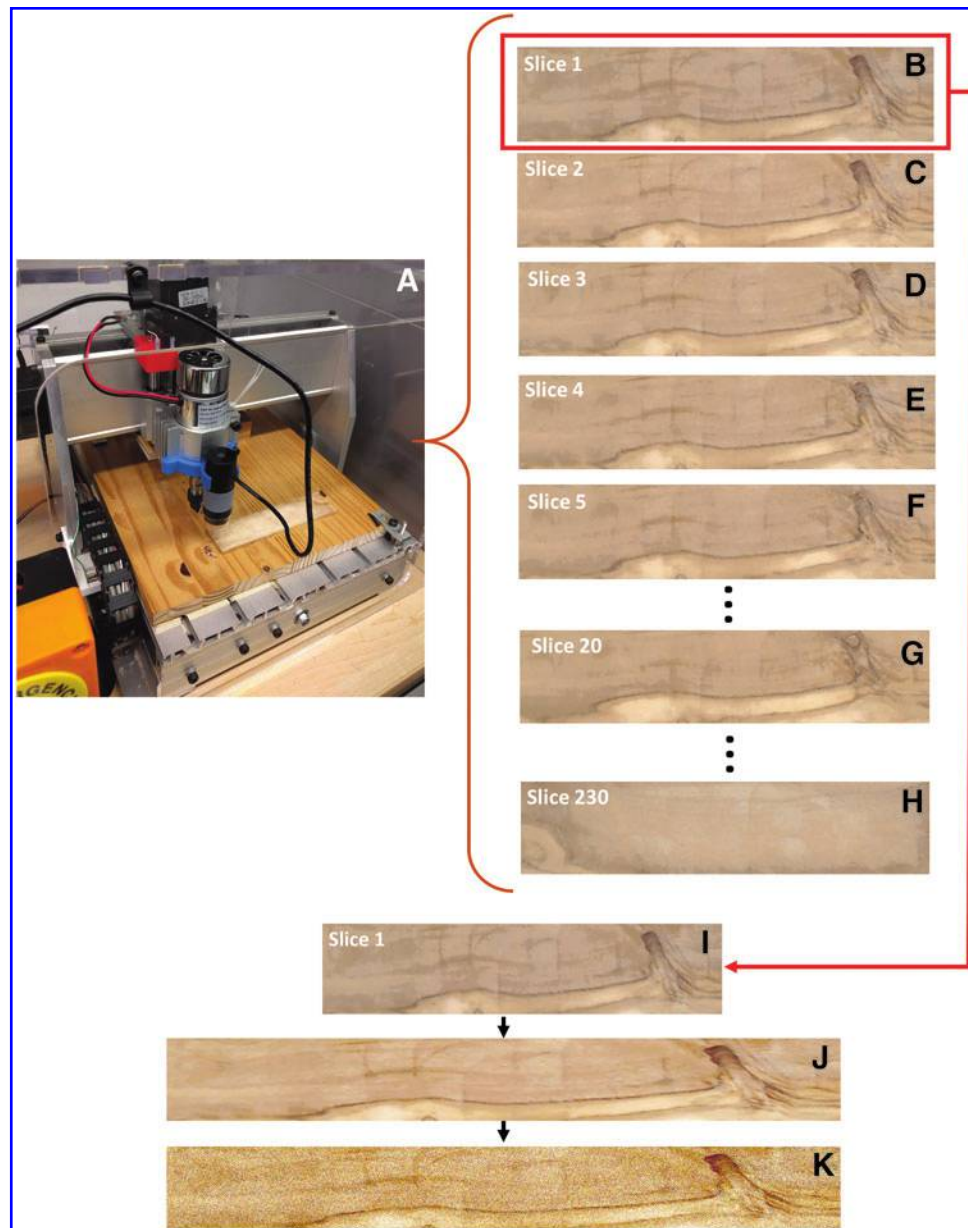


FIG. 2. (A) Destructive imaging setup: a camera-equipped desktop CNC mill and the wooden sample mounted on a baseboard. (B–I) A selection of cropped cross-sections of olive wood slices. (J) Dilated image cross-section to match the aspect ratio of J750 3D printer. (K) Superposed bitmaps assuming no mixing of resin droplets. 3D, three-dimensional; CNC, computer numerical control.

Stochastic dithering

The interpolated RGB images were converted to a CMYK color space to match the primary inks of a Stratasys J750 printer. The mapping from the RGB to CMYK space was performed using a stochastic dithering algorithm implemented in MATLAB.^{17,18} Dithering is often used in computer displays and printers to simulate color transitions. In brief, two adjacent pixels are used to locally simulate the appearance of a third color. For example, a red and a yellow color may dither in a mosaic to produce the appearance of an orange color. Ultimately, a compromise is made between spatial and color resolution to enhance the latter.¹⁹ In this study, stochastic dithering was adopted to maximize the consistency of CMYK images with the RGB color profile. The subroutine used for the stochastic dithering is shown in Table 1. The image shown in Figure 3A served as input for the stochastic dithering script. For each RGB pixel in Figure 3A, a vector of percentages was construed, representing the equivalent composition of the pixel in the CMYK color space. Next, the script created a matrix of the same xy dimensions as the original image, and this matrix was populated with randomly generated values ranging from 0 to 1.

These random values were used to select which CMYK colors mapped to the spatial locations of each pixel. For each image, the script generates six PNG image files, one for each color primitive of the printer. This process of separating an image into bitmaps of its constituent colors is known as color separation²⁰ and is shown in Figure 3. Each of the computed PNG images pertains to a specific CMYK resin, corresponding to cyan, magenta, yellow, black, white, and clear. Each white pixel in the bitmap denotes one voxel being placed on the print tray, whereas black pixels denote voids in the material. As only a single resin drop can represent each voxel, no overlaps between the bitmaps should exist. The superposed images from Figure 3B are shown in Figures 2K and 3C, thus reflecting the printing outcome, assuming no resin mixing.

Printing

To achieve multimaterial printing, the Stratasys J750 printer sputters droplets of dissimilar materials on the build

tray before gently compressing them with a metal roller to effectively mix adjacent droplets. This mixing of resins removes the grittiness seen in Figure 3C to produce smoother, continuous segments shown in Figure 4. After the metal roller passes across a layer, the layer is cured with ultraviolet light, and the machine starts printing the next layer. Generation of support structure is automatically handled by the Stratasys software, and is not evident in the bitmaps.

Results

The wooden blocks were manufactured using the process described in the preceding section, and are shown in Figures 1, 4, and 5. To reveal the internal multicolor structure, the printed blocks in Figure 4A were dipped in liquid nitrogen and shattered, producing the fragments shown in Figure 1. In addition, other blocks were broken using a chisel, as shown in Figure 4B, C. Figures 1 and 4C reveal that the differently colored resins have mixed to form a continuous grain. Thus, it is evident that the printing process is capable of accurately replicating the intricate grains characterizing the structure of the entire wooden block.

Image processing techniques were employed to quantitatively show the difference between a printed layer and the original image in both hue, saturation, value (HSV) and RGB color spaces. The input images of slice 1, the top slice of the sample, are shown in both RGB and HSV color spaces in Figure 3D, G, respectively. Similarly, the output images of the as-printed layer are shown in 3E and 3H. For both HSV and RGB images, mean values were subtracted, and the arrays were then divided by the respective standard deviations to normalize for brightness and contrast. The difference of these normalized images in RGB and HSV format produced the difference images seen in Figure 3F, I, respectively. The L^2 norm of the difference images was calculated. The L^2 norm was chosen as it pertains to root mean square error, a common and well-understood error metric across different disciplines. Furthermore, the L^2 norm is well suited for arbitrarily large arrays, which are intrinsic to voxel printing workflows as seen in this work. For slice 1, as seen in Figure 3D, the L^2 norm was 1.48. When converting the images to HSV format, the L^2 norm of error was 1.31. These norms, while quantitative, are relatively

TABLE 1. PSEUDOCODE SHOWING THE STOCHASTIC DITHERING ALGORITHM FOR ONE LAYER

Algorithm: Stochastic Dithering

Input: JPEG Image

Output: Six CMYKW PNG Images

- 1: Separate input image into Red [R], Green[G], Blue[B] arrays of size $m \times n \times l$.
- 2: Generate $m \times n$ array [R] populated with random values in range of [0,1].
- 3: Generate empty $m \times n$ arrays: Black [K], Cyan [C], Magenta [M], Yellow [Y], White [W].
- 4: Perform initial RGB to CMYK Mapping:
- 5: $K = 1 - \max(R, G, B)$
- 6: $C = (1 - R - K) / (1 - K)$
- 7: $M = (1 - G - K) / (1 - K)$
- 8: $Y = (1 - B - K) / (1 - K)$
- 9: Implement Stochastic Dithering to populate CMYKW arrays:
- 10: If $(R \leq C) \leftarrow 1$, else $C \leftarrow 0$
- 11: If $(R > C)$ & if $(R \leq (C + M)) \leftarrow 1$, else $M \leftarrow 0$
- 12: If $(R > (C + M))$ & if $(R \leq (C + M + Y)) \rightarrow 1$, else $Y \leftarrow 0$
- 13: If $(R > (C + M + Y))$ & if $(R \leq (C + M + Y + K)) \leftarrow 1$, else $K \leftarrow 0$
- 14: If $(R > (C + M + Y + K)) \leftarrow 1$, else $W \leftarrow 0$
- 15: Write six PNG images, one for each primary color, where 1s map to white pixels, and 0s map to black pixels.

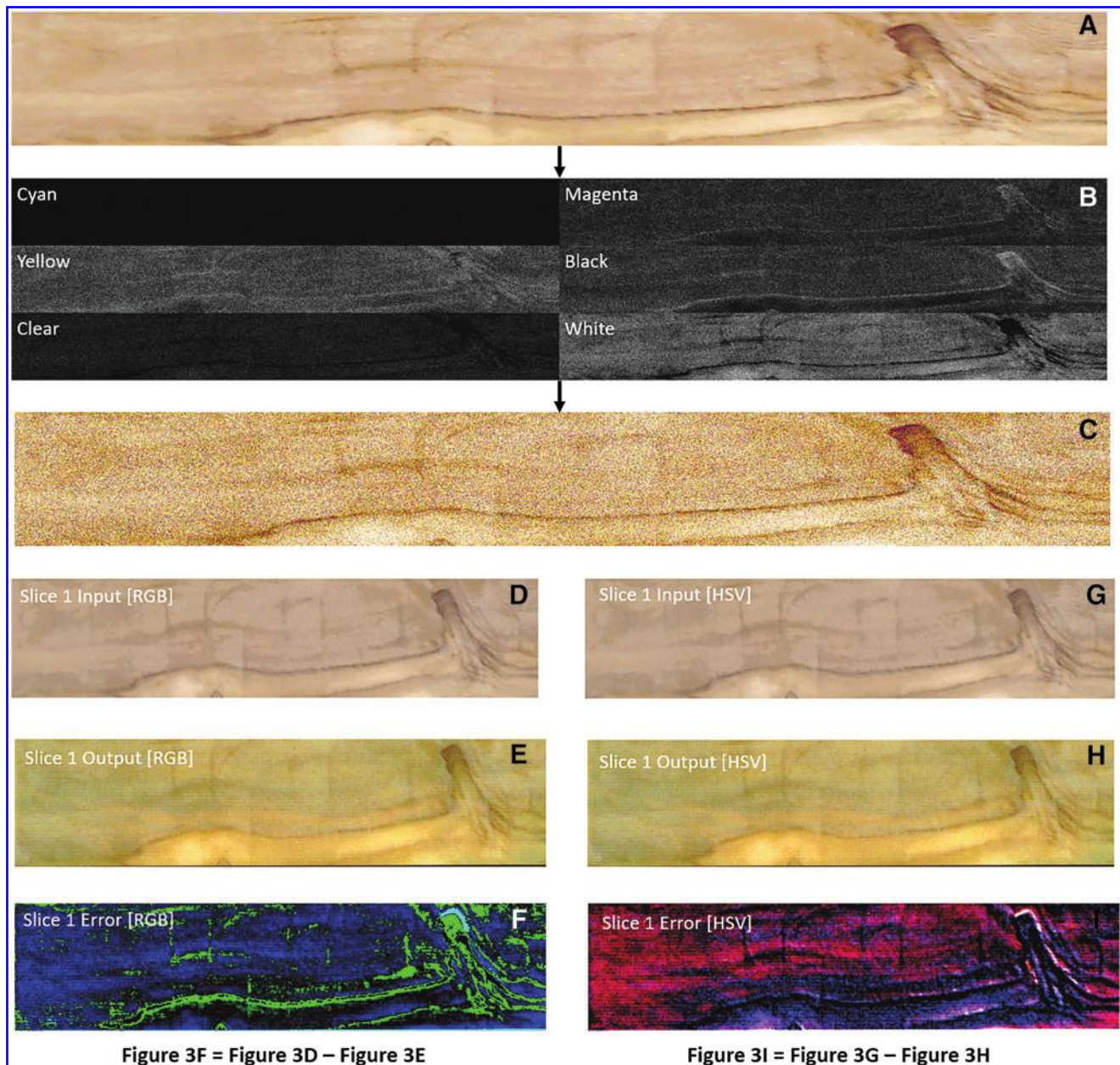


FIG. 3. (A) An original, RGB cropped image of a wooden slice. (B) The image separated into equivalent CMYK constituent pixels. (C) Bitmaps from Figure 2B, superposed using stochastic dithering. (D) Input image of Slice 1 in RGB format. (E) Output image of the as-printed Slice 1 in RGB format. (F) Difference image between 3D and 3E in RGB format. (G) Input image of Slice 1 in HSV format. (H) Output image of the as-printed Slice 1 in HSV format. (I) Difference image between 3D and 3E in HSV format. CMYK, cyan, magenta, yellow, and black; HSV, hue, saturation, value; RGB, red, green, and blue.

arbitrary numbers, and are of most value for comparing images specific to this workflow. Both these error norms can be lowered by performing white balancing on both the input and output images, and by introducing fiducials in both the original wooden part and the replicated part. Fiducials would improve pixel-to-pixel alignment, providing a more accurate error calculation. Future error investigation can borrow image processing and computer vision algorithms to further characterize the errors associated with voxel printing.

In addition to digitally replicating the wooden sample, it was important to investigate how modifiable the bitmap stacks were, as well as establish if this workflow was con-

ducive to arbitrary geometries. To meet these objectives, the color profile of the images was batch edited using Adobe Photoshop, and then reprinted to obtain the part depicted in Figure 5A. A similar grain pattern can be observed, although comprised of a completely different hue. Figure 5B shows the same wooden grain applied to the topologically complex shape of an alligator. This structure was generated by performing a Boolean operation between the STL file of an alligator and a 3D point cloud reconstruction of the olive wood image stack. Ultimately, the two images in Figure 5 show that this workflow can work well for editing anisotropic structures by changing the constituent bitmap image stack. This process

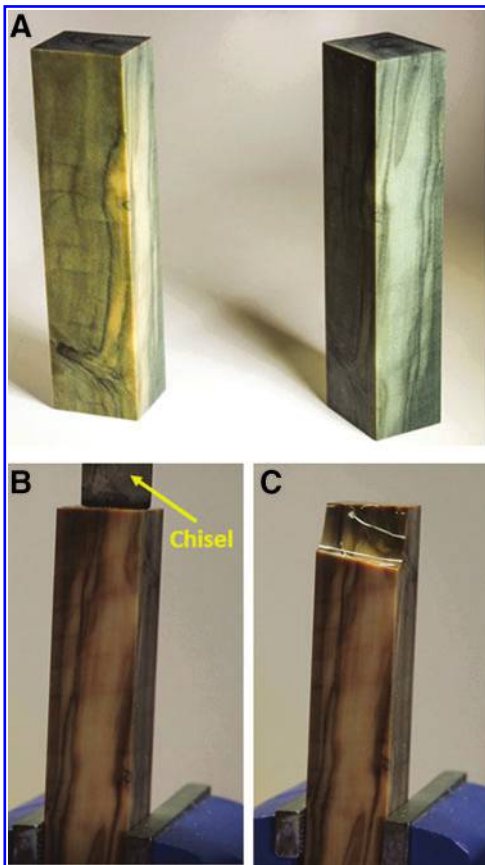


FIG. 4. (A) Two printed wooden blocks, one of which is 15% darker than the other. (B) Wooden block mounted on a vice preloaded with a chisel. (C) Chiseled wooden block showing internal grain structure.

allows designers to embed the internal structure of one object to other arbitrarily complex geometries.

Discussion

While the Stratasys J750 printer has the ability to mix resins of dissimilar durometers, the interaction between dissimilar durometers is highly nonlinear and out of the scope of this study. Thus the presented workflow focused only on one property of texture: color. Other texture properties such as specularities are limited by the mixing mechanics of photoacrylates and the printer resolution, respectively. Nevertheless, the ability to replicate internal grains in color profiles can be extended to replicating stiffness profiles for materials whose physical properties map closely to their visual properties. The ability to take the internal profile of one material and apply it to another has significant implications for both designers and manufacturers. With design spaces that span >760 billion voxels, designers have seemingly boundless design freedom, which not only requires new software tools but also necessitates modification of existing design principles. It is no coincidence that algorithmic, bioinspired designs, which are pervasive in natural phenomena, are well suited to the voxel printing workflow. This is because they are inherently cell-based processes adept at arranging voxel-like patterns to achieve an optimal state. The voxel printing workflow presented in this work can also leverage digital photography tools, such as Photoshop

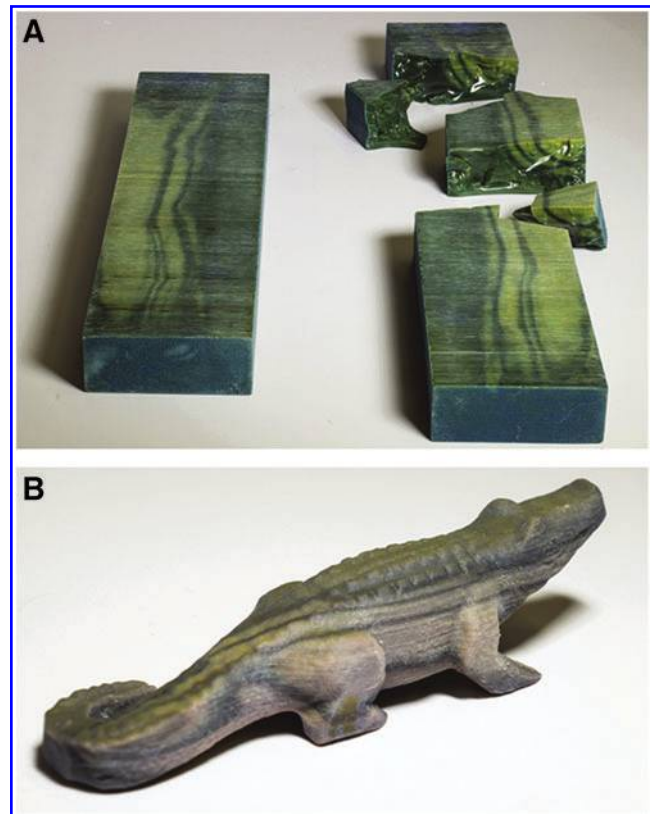


FIG. 5. (A) A modified and digitally replicated piece of wood, cut in half by a bandsaw and then shattered in liquid nitrogen. (B) An alligator shape with the internal grain of the olive wood sample.

or GNU Image Manipulation Program, as these are suited for effective manipulation of large pixel-based arrays. As parts become larger and voxel size declines, the number of voxels will exceed 760 billion per build tray. To keep up with such demands, parallel assembly of voxels is recommended, as this will reduce printing time while making the process economically competitive. PolyJet and Multi Jet Fusion, as the pre-eminent voxel-friendly processes, utilize parallel assembly to sputter out voxels. It is envisaged that this focus on parallel assembly will continue, as printer speed and efficiency increase.

Since voxel-based designs are inherently digital, there is a significant benefit to sharing bitmap stacks of known materials. Just as two-dimensional stock images of wood can be downloaded free of charge, in the future, designers, engineers, and technicians will likely be able to access bitmap stacks, which they will customize to fit their specific design requirements. In support of this goal, we have launched an online repository of destructively imaged wooden samples. The repository contains several types of wood, and can be accessed on the Creative Machines' Lab website.¹⁵ For each sample, the original wooden images are available, along with a GrabCAD voxel print file (GCVF), and the script used to perform stochastic dithering and color separation.

Conclusions

The destructive imaging workflow described in this article can be readily used for any machinable material with resolvable

internal grains. However, destructive imaging is both energy and time consuming, and renders the original sample unusable. To aid imaging efficacy and accuracy, materials can be treated with fluorescent dyes to expose material properties, and voxel maps can also be postprocessed by using appropriate software tools to filter out noise or tooling marks. Voxel maps produced by such software can also be corrected to correlate with vetted coupons of material.

The workflow presented in this study could also benefit from less invasive imaging techniques, such as magnetic resonance imaging, MR enterography, X-ray, or infrared. A combination of such techniques can be used for metals, organic materials, and composites. Further information can be gleaned by cross-referencing data obtained from different techniques such as thermal, mechanical, acoustic, and electrical imaging. Nondestructive imaging will be particularly beneficial for larger parts that need adaptive resolution, and may be cumbersome and time prohibitive to machine.

The voxel printing workflow does not necessarily need point clouds generated from imaging techniques. It is possible to entirely generate point clouds through software, as in the case of fractal-inspired materials. Previous work in this domain suggests the potential for using fractal-inspired materials, which presently cannot be manufactured.^{20,21} Voxel printing is well positioned to bring many of these fractal-based materials from the virtual into the physical realm. It is worth noting that voxel-printed objects comprised of dissimilar materials can exhibit significant nonintuitive anisotropies,²² which can be challenging to simulate. Thus, judicious use of testing and simulation is needed to predict their behavior and inform the production of algorithmically designed materials.

While this work focused on digital reproducibility of wood, the same approach can be applied to many other anisotropic materials. Moreover, this study has shown the ability to “photoshop” 3D structures to change color along with the potential for applying internal structures to arbitrarily complex shapes.

Acknowledgments

The authors thank Ohad Meyuhas and Jesse Roitenberg from Stratasys Limited for their insight and dedication to PolyJet voxel printing technology. The company’s support has enabled the use of the J750 3D printer employed in this study. The authors also acknowledge Jonathan Blutinger for his photographs of printed samples.

Author Disclosure Statement

No competing financial interests exist.

References

1. HP Multi Jet Fusion Technology. HP Development Company, L.P. 4AA5-5472EEW, October 2016, Rev 6. Available at <http://www8.hp.com/us/en/printers/3d-printers.html> (accessed April 14, 2018).
2. Design With Brilliance: Game Changing Versatility and Realism with the World’s Most Advanced 3D Printer. 2016. Available at www.stratasys.com/resources/search/ebooks/j750 (accessed April 14, 2018).
3. Hiller J, Lipson H. Tunable digital material properties for 3D voxel printers. *Rapid Prototyp J* 2010;16:241–247.
4. Chiu WK, Yu KM. Direct digital manufacturing of three dimensional functionally graded material objects. *Comput Aided Des* 2008;40:1080–1093.
5. Lipson H, Kurman M. Designing the future. In: *Fabricated: The New World of 3D Printing*. John Wiley & Sons, New York, NY, 2013; pp.100–101.
6. ASTM. F2792. 2012. Standard terminology for additive manufacturing technologies. ASTM F2792-10e1: pp. 6.
7. Wohlers T. Wohlers Report 2018, Additive Manufacturing State of the Industry. Wohlers Associates, Inc., Fort Collins, 2018.
8. Doubrovski EL, Tsai EY, Dikovsky D, *et al.* Voxel-based fabrication through material property mapping: A design method for bitmap printing. *Comput Aided Des* 2008;40:1080–1093.
9. Bader C, Kolb D, Weaver J. Data-driven material modeling with functional advection for 3D printing of materially heterogeneous objects. *3D Print Addit Manufact* 2016;3:74–77.
10. Oxman N, Tsai E, Firstenberg M. Digital anisotropy: A variable elasticity rapid prototyping platform. *J Virtual Phys Prototyp* 2012;7:261–274.
11. Aage N, Andreassen E, Lazarov SB. Giga-voxel computational morphogenesis for structural design. *Nature* 2017; 550:84–86.
12. Autodesk, Inc. Available at <https://www.autodesk.com/products/netfabb/features> (accessed April 14, 2018).
13. Mici J, Rothenberg B, Brisson E, *et al.* Optomechanical performance of 3D-printed mirrors with embedded cooling channels and substructures. *Proceeding of SPIE Vol. 9573, Optomechanical Engineering 2015, 957306*. SPIE Bellingham, WA, 2015.
14. Hiller J, Lipson H. Dynamic simulation of heterogeneous printed objects. 2012;arXiv:1212.2845.
15. Creative Machines Laboratory, Columbia University. Available at <https://www.creativemachineslab.com/open-source.html> (accessed February 1, 2018).
16. The MathWorks, Inc. Nearest Neighbor, Bilinear, and Bicubic Interpolation Methods. Available at <https://www.mathworks.com/help/vision/ug/interpolation-methods.html> (accessed May 17, 2018).
17. Akarun L, Yardimci Y, Cetin AE. Adaptive methods for dithering color images. *Proceedings of the International Conference on Image Processing, Washington, DC, 1995*.
18. Babaei V, Vidimce K, Foshey M. Color contouring for 3D printing. *ACM Trans Graph* 2017;36:124.1–124.15.
19. Stone C, Cowan W, Beatty, JC. Color spaces for gamut mapping. *Color Gamut Map* 1988;7:249–292.
20. Cho Y, Shin JH, Costa A, *et al.* Engineering the shape and structure of materials by fractal cut. *Proc Natl Acad Sci USA* 2014;111:17390–17395.
21. Vaithilingam J, Saleh E, Korner L. 3-Dimensional inkjet printing of macro structures from silver nanoparticles. *Mater Des* 2018;139:81–88.
22. Dikovsky D. Multi-material 3D Printing. Stratasys, Ltd., 2014. Rosemont, IL: RadTech UV & EB Tech Expo.

Address correspondence to:

Joni Mici
 Department of Mechanical Engineering
 Columbia University
 100 Morningside Drive, No. 2M
 New York, NY 10027

E-mail: joni.mici@columbia.edu